

Dramatic Enhancement of CO₂ Uptake by Poly(ethyleneimine) Using Zirconosilicate Supports

Yasutaka Kuwahara,^{†,‡} Dun-Yen Kang,[†] John R. Copeland,[†] Nicholas A. Brunelli,[†] Stephanie A. Didas,[†] Praveen Bollini,[†] Carsten Sievers,[†] Takashi Kamegawa,[‡] Hiromi Yamashita,[‡] and Christopher W. Jones^{*,†}

[†]School of Chemical & Biomolecular Engineering, Georgia Institute of Technology, 311 Ferst Drive, Atlanta, Georgia 30332, United States

[‡]Division of Materials and Manufacturing Science, Graduate School of Engineering, Osaka University, 2-1 Yamada-oka, Suita, Osaka 565-0871, Japan

S Supporting Information

ABSTRACT: The CO₂ adsorption characteristics of prototypical poly(ethyleneimine)/silica composite adsorbents can be drastically enhanced by altering the acid/base properties of the oxide support via incorporation of Zr into the silica support. Introduction of an optimal amount of Zr resulted in a significant improvement in the CO₂ capacity and amine efficiency under dilute (simulated flue gas) and ultradilute (simulated ambient air) conditions. Adsorption experiments combined with detailed characterization by thermogravimetric analysis, temperature-programmed desorption, and in situ FT-IR spectroscopy clearly demonstrate a stabilizing effect of amphoteric Zr sites that enhances the adsorbent capacity, regenerability, and stability over continued recycling. It is suggested that the important role of the surface properties of the oxide support in these polymer/oxide composite adsorbents has been largely overlooked and that the properties may be even further enhanced in the future by tuning the acid/base properties of the support.

Concern about the increasing atmospheric CO₂ concentration and its impact on the environment has led to increasing attention directed toward finding advanced materials/technologies suited for efficient carbon capture and storage (CCS).^{1–5} As a traditional gas separation technology, adsorption of CO₂ using a variety of different types of solid materials has been investigated.⁶ Among the various materials, silica-supported amines⁷ (e.g., amine-impregnated porous silicas,^{8,9} amine-grafted silica materials,¹⁰ and hyperbranched aminosilica materials¹¹) offer outstanding capture performance at low temperature and are therefore promising candidates for postcombustion capture of CO₂ from large stationary sources such as flue gas (ca. 10% CO₂) or ambient air³ (ca. 400 ppm CO₂, “air capture”¹²).

To date, silica has been used as the support material in the overwhelming majority of preparations of amine/oxide composite adsorbents.⁷ Examples of the use of other oxides such as alumina,¹³ titania,¹⁴ or composite oxides such as aluminosilicates^{8b,15} or titanosilicates¹⁶ are rare. Indeed, the predominant focus of researchers to date has been on adjusting the porosity of the silicate support^{9,10,11d,17} and altering the nature of the amine groups.^{10–12} However, there is a significant

untapped opportunity to improve the adsorption characteristics by manipulating the intrinsic properties of the support, such as the acidity or basicity.

One of the advantageous characteristics of silicate materials is the ability to create tunable porous solids via the introduction of heteroatoms (e.g., Al, Ti, and Zr) into the silica matrix by direct or postsynthetic procedures.^{18,19} It is expected that electrophilic/nucleophilic sites created in this way can play a role in CO₂ adsorption by acting as CO₂ or amine activating sites. For example, Ratnasamy and co-workers reported that adenine-grafted Ti-SBA-15 can efficiently catalyze the cycloaddition of CO₂ with epoxides as a result of its improved acid/base properties, coupling the Lewis acidity of the Ti sites with the basicity of the grafted amines.²⁰ Subsequently, Young and Notestein¹⁶ reported that aminopropyl-grafted silica including Ti sites spatially isolated from amine sites gives a material where both sites (i.e., Brønsted base and Lewis acid, respectively) retain their ability to perform independent chemistry. We hypothesized that the introduction of such sites onto aminopolymer-impregnated porous silica systems may also provide productive synergism at the interface between the aminopolymer and the solid surface, thus accordingly providing improved CO₂ adsorption performance.

In this communication, we report an outstanding enhancement of the CO₂ uptake of prototypical (class 1)^{7–9} amine-based solid adsorbents composed of low-molecular-weight branched poly(ethyleneimine) (PEI) impregnated into SBA-15 mesoporous silica when the silica support contains isolated Zr species within the framework. PEI was used as the amine source because of its high amine density and accessible primary amine sites on chain ends.²¹ Zr atoms were chosen as the heteroatom species on the basis of a preliminary survey demonstrating that Zr substitution²² created more effective amine-stabilizing sites on the silica surface compared with Ti or other common heteroatoms. Indeed, the substitution of Zr atoms into the silicate matrix allows for the creation of organic/inorganic composite adsorbents with dramatically enhanced CO₂ adsorption performance (as a function of Zr loading) using mixed gases simulating both traditional flue gas capture and CO₂ removal from ultradilute gas streams such as ambient air.³

Received: April 1, 2012

Published: June 15, 2012



Table 1. Textural Properties and CO₂ Adsorption Capacities of PEI/Zr-SBA-15 Materials

Adsorbent	Zr/Si ^a		PEI loading ^b (wt%)	Amine content (mmol N/g)	without PEI			with PEI			Occupancy rate ^f (%)	CO ₂ adsorption ^g	
	gel	product			S _{BET} ^c (m ² /g)	V _{total} ^d (cm ³ /g)	d _p ^e (nm)	S _{BET} ^c (m ² /g)	V _{total} ^d (cm ³ /g)	d _p ^e (nm)		400 ppm (mmol CO ₂ /g)	10% (mmol CO ₂ /g)
PEI/SBA-15	-	-	30.8	7.40	683	1.19	8.5	242	0.639	7.3	35	0.19	0.65
PEI/Zr4-SBA-15	0.05	0.038	33.0	7.92	642	1.08	8.6	205	0.460	7.3	43	0.64	1.34
PEI/Zr7-SBA-15	0.10	0.070	34.7	8.33	647	1.23	9.5	230	0.613	7.8	41	0.85	1.56
PEI/Zr11-SBA-15	0.15	0.109	33.1	7.95	601	0.692	7.0	101	0.179	5.8	67	0.83	1.41
PEI/Zr14-SBA-15	0.20	0.138	34.5	8.28	510	0.395	4.4	<1.0	<0.01	N.D. ^h	124	0.26	0.24

^aDetermined by elemental analysis. ^bDetermined by TGA. ^cCalculated from the adsorption branch of the N₂ isotherm. ^dValues at P/P₀ = 0.99. ^eEstimated by the BdB–FHH (Frenkel–Halsey–Hill-modified Broekhoff–de Boer) method. ^fDefined by the equation [occupancy rate (%)] = [calculated aminopolymer volume (cm³_{polymer}/gSiO₂)]/[V_{total} of bare adsorbent (cm³/g)] × 100%, assuming a PEI density of 1.07 cm³/g. ^gMeasured at 25 °C under dry conditions (adsorption time 12 h). ^hN.D. = not determined.

The synthesis of Zr-SBA-15 materials with varied Zr content (ZrX-SBA-15, X = 0–14 mol % relative to Si) was performed according to a previous report.²³ The structures of the obtained calcined Zr-SBA-15 materials with Zr/Si molar ratios of 0.038–0.138 were characterized by means of X-ray diffraction (XRD), N₂ physisorption, and transmission electron microscopy (TEM), which identified the materials as having periodic 2D hexagonal mesoporous structures (*P6mm*) with large Brunauer–Emmett–Teller (BET) surface areas ($S_{\text{BET}} \approx 650$ m²/g), large pore volumes ($V_p \approx 1.2$ cm³/g), and uniform pore sizes ($d_p \approx 9$ nm) for the unmodified SBA-15, Zr4-SBA-15, and Zr7-SBA-15 [Table 1; also see Figures S1–S4 in the Supporting Information (SI)]. However, partial collapse of the mesostructure with appreciable loss of surface area and pore volume was observed when more than 15 mol % Zr was used. Zr K-edge X-ray absorption fine structure (XAFS) coupled with XRD and Fourier transform Raman spectroscopy confirmed that the Zr species are mostly present as highly dispersed and isolated sites within the silica framework in all cases, but they cause a distortion of the silica network accompanied by creation of silica defect sites such as silanols with increasing Zr content (Figures S5 and S6). In addition, the effective charge of Zr was determined to be ca. 4+ in all cases on the basis of the absorption-edge energies in the XAFS spectra (see the discussion of Figure S5 on p S10 in the SI). These combined characterization results indicate that Zr atoms are effectively covalently embedded within the silica matrix via isomorphous substitution irrespective of the Zr content, although the introduction of >15 mol % Zr leads to disordering of the mesostructure and results in reduced mesoporosity.

A series of PEI/Zr-SBA-15 composite materials was prepared by physical impregnation of a low-molecular-weight PEI (MW = 800 Da) into the calcined Zr-SBA-15 samples using MeOH as the solvent, in which the organic content was adjusted to ca. 30 wt % for all of the samples. While larger adsorption capacities could undoubtedly be obtained using higher amine loadings (e.g., ca. 50 wt %),^{8,9,17a} a more moderate loading was chosen here to promote close contact between the PEI and the solid surface while still providing appreciable sample porosity. Thermogravimetric analysis (TGA) confirmed the intended PEI loading levels in all cases, and on this basis the amine loadings and occupancy rates were stoichiometrically calculated. As summarized in Table 1, PEI-impregnated SBA-15, Zr4-SBA-15, and Zr7-SBA-15 retained their ordered mesoporosity and sufficient pore volume that they could be considered porous

adsorbents. In contrast, complete pore saturation was observed for PEI/Zr14-SBA-15 because of its smaller pore volume.

The CO₂ adsorption performance of the PEI/Zr-SBA-15 composites was analyzed by exposing the solids to either a 10% or 400 ppm CO₂/Ar flow at a rate of 100 mL/min (both under dry conditions) in a thermogravimetric analyzer. The CO₂ uptakes of the conventional PEI/SBA-15 were 0.19 and 0.65 mmol/g at 400 ppm and 10% CO₂, respectively. This sample provided the baseline performance to which the Zr-substituted samples were compared.²⁴ The series of PEI/Zr-SBA-15 composite materials showed significantly increased CO₂ capacities and thus higher amine efficiencies under both dilute and ultradilute CO₂ conditions up to a Zr/Si ratio of 0.11 (Figure 1). The highest CO₂ uptake was attained for PEI/Zr7-

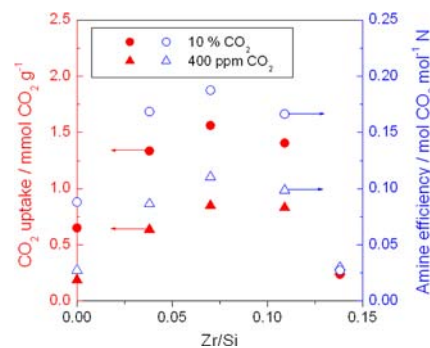


Figure 1. CO₂ adsorption capacities (solid symbols) and amine efficiencies (open symbols) of 30 wt % PEI-impregnated Zr-SBA-15 materials as a function of Zr/Si molar ratio of the support. The reported values are pseudoequilibrium capacities measured at 25 °C under dry conditions (adsorption time was fixed at 12 h).

SBA-15, which showed amine efficiencies 2.1 times and 4.0 times higher than the conventional PEI/SBA-15 material under identical 10% and 400 ppm CO₂ conditions, respectively. Zr7-SBA-15 exhibited the highest adsorption capacity over a range of temperatures as well (Figure S7). These results clearly demonstrate the material's outstanding CO₂ adsorption performance, especially from ultradilute gas. Meanwhile, the inclusion of greater amounts of Zr in the silica led to reduced CO₂ uptake and decreased amine efficiency. This trend coincides with the changes in the support structure induced by larger Zr concentrations, as observed by structural analyses (see above). It is well-documented that the CO₂ capacity of these types of materials is strongly dependent on several structural factors, such as the pore diameter, remaining pore

volume, and aminopolymer loading.^{8,9} In this regard, the decreased performance of the PEI/Zr14-SBA-15 sample can be clearly associated with the poor structural characteristics of the support (e.g., surface area, porosity, etc.). In contrast, the PEI loading, calculated occupancy rates, and structural parameters of the PEI/SBA-15, PEI/Zr4-SBA-15, and PEI/Zr7-SBA-15 adsorbents were all quite similar (see Table 1), yet the latter two materials presented significantly increased adsorption performance. This unambiguously demonstrates the positive effect of moderate levels of Zr incorporation in the silicate matrix on the CO₂ adsorption properties. In contrast, Young and Notestein demonstrated that Ti sites present on the silica support surface diminish the ability of the amines to adsorb CO₂ if the aminopropyl groups are directly grafted on its surface, since the Ti sites interact with amines by acting as Lewis acid sites.¹⁶ These reports, coupled with the fact that the entire support surface is likely covered with aminopolymer in our case, led us to the hypothesis that strong, productive interactions between the PEI and Zr-containing oxide surface enhanced the ability of some of the amines to capture CO₂. This hypothesis is supported by TGA and IR analyses. The PEI decomposition temperature determined by TGA shifted to 30 °C higher temperatures on the Zr-SBA-15 materials relative to traditional pure silica SBA-15 (Figure S8). A significant shift was also observed in FT-IR spectra, whereby several peak shifts assignable to NH₂ and CH₂ deformations of the PEI polymer were observed after impregnation onto the SBA-15 supports. Specifically, the former peak shift was more pronounced when Zr7-SBA-15 was used as the support (Figure S9). These results suggest that the immobilized PEI interacts with the Zr-SBA-15 surface differently than with pure-silica SBA-15.

To provide a quantitative understanding of the effect of the incorporated Zr heteroatoms on the CO₂ adsorption, the measured CO₂ adsorption capacities of PEI/Zr-SBA-15 materials were plotted as a function of the surface density of the acid and base centers (Figure S10), which were determined by NH₃ and CO₂ temperature-programmed desorption (TPD) analysis, respectively (for the TPD profiles, see Figure S11). As the Zr content was increased from 0 to 0.11 mol %, both the surface acid and base densities increased in a roughly linear fashion, and distinct correlations between the measured CO₂ capacities and the surface acid and base densities were observed under both adsorption conditions (10% and 400 ppm CO₂ in inert gas). While Zr14-SBA-15 also possesses acid/base bifunctionality comparable to the other supports containing moderate amounts of Zr (Zr4-SBA-15 and Zr7-SBA-15), it deviated from these correlations because of its subpar porosity characteristics. At this stage of the work, it is too early to draw unambiguous conclusions concerning the molecular-level basis of the CO₂ adsorption capacity improvement upon incorporation of moderate levels of Zr in the silicate framework, but a plausible explanation arises via stabilizing interactions between the aminopolymer and the amphoteric zirconosilicate support.

On the basis of the above hypotheses, we further carried out in situ FT-IR experiments to clarify the CO₂ adsorption/desorption kinetics on the adsorbents. In situ FT-IR difference spectra upon CO₂ adsorption (Figure 2A) showed that PEI/Zr7-SBA-15, the adsorbent with the best CO₂ capacity among those examined, allowed for more efficient adsorption of CO₂ at low pressure with higher CO₂ capacity compared with conventional PEI/SBA-15. Although bare Zr7-SBA-15 was shown to have a trace CO₂ adsorption capacity, it accounts for only 1% of the total CO₂ capacity of PEI/Zr7-SBA-15 (see

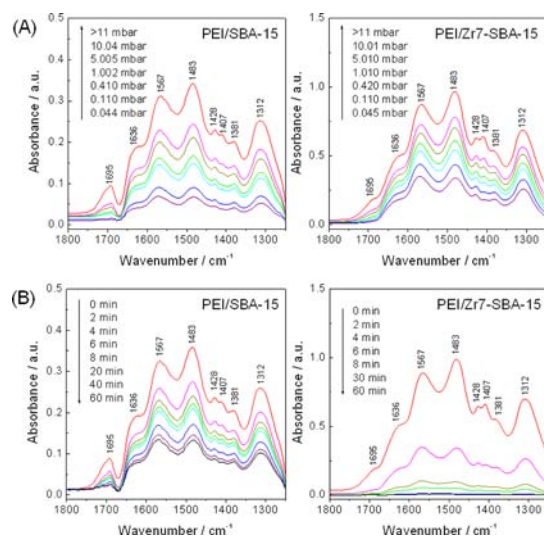


Figure 2. In situ FT-IR difference spectra of (A) CO₂ adsorbed on PEI/SBA-15 and PEI/Zr7-SBA-15 at increasing CO₂ pressures and (B) CO₂ desorbed from CO₂-saturated PEI/SBA-15 and PEI/Zr7-SBA-15 as a function of under applied vacuum time.

Figure S12), thereby ruling out the possibility that direct interaction between CO₂ and surface Zr sites drives the enhanced adsorption. In regard to the CO₂ adsorption sites, the observed absorption bands were all typical of those previously reported on conventional amine-based adsorbents,²⁵ indicating that the amine groups in PEI are the main adsorption sites for CO₂. The most noticeable differences observed via FT-IR were in the difference spectra upon CO₂ desorption (Figure 2B). PEI/Zr7-SBA-15 allowed for rapid, nearly complete CO₂ desorption within a short time period of applied vacuum (even at room temperature), compared with the traditional PEI/SBA-15 sorbent. In the case of the conventional adsorbent, some fraction of the CO₂ adsorbed could not be eliminated even after a prolonged period of vacuum at room temperature, indicating limited adsorption reversibility of the PEI in silica, perhaps due to aggregation/degradation of the PEI during the CO₂ adsorption. This is consistent with color changes of the adsorbent after multiple adsorption/desorption cycles. The PEI/SBA-15 changed from white to yellow after cycling, suggesting substantial degradation/aggregation of the PEI, whereas PEI supported on Zr7-SBA-15 remained white even after repeated use. From the combined data, we conclude that Zr atoms incorporated into the silicate stabilize the PEI, yielding enhanced adsorption capacities and limiting undesired degradation/aggregation of PEI.

Figure 3 compares the CO₂ adsorption capacities of the conventional PEI/SBA-15 and PEI/Zr7-SBA-15 composites over four adsorption/desorption cycles at 25 °C with 400 ppm CO₂/Ar flow, in which the CO₂ was desorbed from the surface in a pure Ar atmosphere at 110 °C for 3 h. The CO₂ capacity of PEI/SBA-15 decreased significantly during moderate cycling; the adsorption capacity decreased by 34% after four cycles, showing that the conventional PEI/SBA-15 adsorbent has limited stability under these bone-dry conditions. This continual capacity reduction may be associated with the loss of CO₂ adsorption sites, perhaps caused by amine degradation originating from urea formation,^{10c,26} by amine loss, or by thermal conformational changes of the PEI during its repeated use. In contrast, the PEI/Zr7-SBA-15 composite, which was

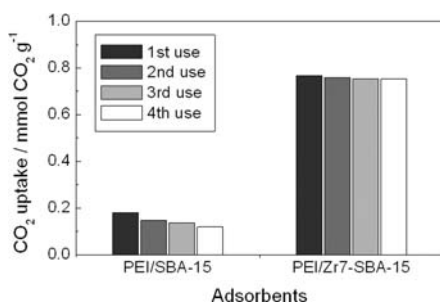


Figure 3. Temperature-swing multicycle CO₂ adsorption/desorption testing of PEI/SBA-15 and PEI/Zr7-SBA-15. The CO₂ capacities under dry conditions at 25 °C using simulated ambient air (400 ppm CO₂) and regeneration under an Ar flow at 110 °C are shown.

shown here to efficiently capture CO₂, adsorbed CO₂ reversibly in a temperature-swing process while retaining most of its CO₂ capacity during the same number of cycles (decreased by 2% after four cycles), demonstrating promising regenerability. These results support our conclusion that Zr atoms on the silica surface efficiently stabilize PEI, providing thermal stability and adsorbent longevity.

In summary, incorporation of Zr species into mesoporous silica has been shown to create a support material for low-molecular-weight polymeric amines that affords composite adsorbents with dramatically enhanced CO₂ adsorption properties. Whereas most work on this class of adsorbent materials (class 1 materials^{7–9}) has focused on employing larger amounts of aminopolymer, different types of aminopolymer,²¹ or silica supports with altered porosities, we have demonstrated here that the acid/base properties of the support play a critical, previously unrecognized role in creating more efficient adsorbents. The combination of adsorption experiments and detailed physicochemical characterization has shown that these new adsorbents containing an optimal amount of Zr (Zr/Si ≈ 0.07) offer significantly increased CO₂ adsorption capacities, improved desorption kinetics, and enhanced thermal stability and regenerability compared with conventional PEI/SBA-15 materials.

■ ASSOCIATED CONTENT

Ⓢ Supporting Information

Materials synthesis; experimental methods; “air capture”; XRD; N₂ adsorption; NH₃/CO₂ TPD; XAFS, Raman, and IR spectra; and CO₂ adsorption. This material is available free of charge via the Internet at <http://pubs.acs.org>.

■ AUTHOR INFORMATION

Corresponding Author

cjones@chbe.gatech.edu

Notes

The authors declare no competing financial interest.

■ ACKNOWLEDGMENTS

This work was financially supported by the New-Vision Professorship awarded to C.W.J. Y.K. thanks the Research Fellowships of the Japan Society for the Promotion of Science (JSPS) for Young Scientists.

■ REFERENCES

- (1) Haszeldine, R. S. *Science* **2009**, *325*, 1647.
- (2) Keith, D. W. *Science* **2009**, *325*, 1654.

- (3) Jones, C. W. *Annu. Rev. Chem. Biomol. Eng.* **2011**, *2*, 31.
- (4) Bhowan, A. S.; Freeman, B. C. *Environ. Sci. Technol.* **2011**, *45*, 8624.
- (5) Hunt, A. J.; Sin, E. H. K.; Marriott, R.; Clark, J. H. *ChemSusChem* **2010**, *3*, 306.
- (6) For reviews, see: (a) Choi, S.; Drese, J. H.; Jones, C. W. *ChemSusChem* **2009**, *2*, 796. (b) D'Alessandro, D. M.; Smit, B.; Long, J. R. *Angew. Chem., Int. Ed.* **2010**, *49*, 6058.
- (7) Bollini, P.; Didas, S. A.; Jones, C. W. *J. Mater. Chem.* **2011**, *21*, 15100.
- (8) (a) Xu, X.; Song, C.; Andresen, J. M.; Miller, B. G.; Scaroni, A. W. *Energy Fuels* **2002**, *16*, 1463. (b) Xu, X.; Song, C.; Andrésen, J. M.; Miller, B. G.; Scaroni, A. W. *Microporous Mesoporous Mater.* **2003**, *62*, 29. (c) Ma, X.; Wang, X.; Song, C. *J. Am. Chem. Soc.* **2009**, *131*, 5777.
- (9) (a) Yue, M. B.; Sun, L. B.; Cao, Y.; Wang, Y.; Wang, Z. J.; Zhu, J. H. *Chem.—Eur. J.* **2008**, *14*, 3442. (b) Heydari-Gorji, A.; Belmabkhout, Y.; Sayari, A. *Langmuir* **2011**, *27*, 12411.
- (10) (a) Franchi, R. S.; Harlick, P. J. E.; Sayari, A. *Ind. Eng. Chem. Res.* **2005**, *44*, 8007. (b) Belmabkhout, Y.; Serna-Guerrero, R.; Sayari, A. *Ind. Eng. Chem. Res.* **2010**, *49*, 359. (c) Sayari, A.; Belmabkhout, Y. *J. Am. Chem. Soc.* **2010**, *132*, 6312.
- (11) (a) Hicks, J. C.; Drese, J. H.; Fauth, D. J.; Gray, M. L.; Qi, G.; Jones, C. W. *J. Am. Chem. Soc.* **2008**, *130*, 2902. (b) Drese, J. H.; Choi, S.; Lively, R. P.; Koros, W. J.; Fauth, D. J.; Gray, M. L.; Jones, C. W. *Adv. Funct. Mater.* **2009**, *19*, 3821. (c) Choi, S.; Drese, J. H.; Eisenberger, P. M.; Jones, C. W. *Environ. Sci. Technol.* **2011**, *45*, 2420. (d) Drese, J. H.; Choi, S.; Didas, S. A.; Bollini, P.; Gray, M. L.; Jones, C. W. *Microporous Mesoporous Mater.* **2012**, *151*, 231.
- (12) See the SI for a brief discussion of CO₂ capture from ambient air.
- (13) (a) Plaza, M. G.; Pevida, C.; Arias, B.; Feroso, J.; Arenillas, A.; Rubiera, F.; Pis, J. J. *J. Therm. Anal. Calorim.* **2008**, *92*, 601. (b) Chaikittisilp, W.; Kim, H. J.; Jones, C. W. *Energy Fuels* **2011**, *25*, 5528. (c) Chen, C.; Ahn, W. S. *Chem. Eng. J.* **2011**, *166*, 646.
- (14) Knöfel, C.; Martin, C.; Hornebecq, V.; Llewellyn, P. L. *J. Phys. Chem. C* **2009**, *113*, 21726.
- (15) Bellussi, G.; Broccia, P.; Carati, A.; Millini, R.; Pollesel, P.; Rizzo, C.; Tagliabue, M. *Microporous Mesoporous Mater.* **2011**, *146*, 134.
- (16) Young, P. D.; Notestein, J. M. *ChemSusChem* **2011**, *4*, 1671.
- (17) (a) Son, W. J.; Choi, J. S.; Ahn, W. S. *Microporous Mesoporous Mater.* **2008**, *113*, 31. (b) Heydari-Gorji, A.; Yang, Y.; Sayari, A. *Energy Fuels* **2011**, *25*, 4206.
- (18) For reviews, see: (a) Sayari, A. *Chem. Mater.* **1996**, *8*, 1840. (b) Corma, A. *Chem. Rev.* **1997**, *97*, 2373. (c) Yamashita, H.; Mori, K. *Chem. Lett.* **2007**, *36*, 348.
- (19) Kuwahara, Y.; Nishizawa, K.; Nakajima, T.; Kamegawa, T.; Mori, K.; Yamashita, H. *J. Am. Chem. Soc.* **2011**, *133*, 12462.
- (20) Srivastava, R.; Srinivas, D.; Ratnasamy, P. *J. Catal.* **2005**, *233*, 1.
- (21) Chaikittisilp, W.; Khunsupat, R.; Chen, T. T.; Jones, C. W. *Ind. Eng. Chem. Res.* **2011**, *50*, 14203.
- (22) For early examples of Zr incorporation into mesoporous silica, see: (a) Newalkar, B. L.; Olanrewaju, J.; Komarneni, S. *J. Phys. Chem. B* **2001**, *105*, 8356. (b) Jones, D. J.; Jiménez-Jiménez, J.; Jiménez-López, A.; Maireles-Torres, P.; Olivera-Pastor, P.; Rodríguez-Castellón, E.; Rozière, J. *Chem. Commun.* **1997**, 431.
- (23) Chen, S. Y.; Jang, L. Y.; Cheng, S. *Chem. Mater.* **2004**, *16*, 4174.
- (24) The adsorption capacities were slightly lower than others reported for related materials (see refs 8, 9, and 11), but the experiments here were all conducted under bone-dry conditions with moderate PEI loadings. Humid conditions could increase the amine efficiency (see refs 6a and 7).
- (25) For more detailed IR peak assignments, see: (a) Wang, W.; Schwartz, V.; Clark, J. C.; Ma, X.; Overbury, S. H.; Xu, X.; Song, C. *J. Phys. Chem. C* **2009**, *113*, 7260. (b) Bacsik, Z.; Atluri, R.; Garcia-Bennett, A. E.; Hedin, N. *Langmuir* **2010**, *26*, 10013. (c) Danon, A.; Stair, P. C.; Weitz, E. *J. Phys. Chem. C* **2011**, *115*, 11540.
- (26) Drage, T. C.; Arenillas, A.; Smith, K. M.; Snape, C. E. *Microporous Mesoporous Mater.* **2008**, *116*, 504.